CERN/LHCC 98-39
LEB Status Report/RD48
21 October 1998

2ND RD48 STATUS REPORT

The ROSE Collaboration
(R&d On Silicon for future Experiments)

Co-Spokespersons: Francois Lemeilleur, Gunnar Lindstroem, Steve Watts

Bari University, Italy
V. Augelli, M. Angarano, D. Creanza, M. De Palma, L. Schiavulli

Berkeley, University of California, Dept. of Materials Science, USA
E. Weber, H. Feick

Brookhaven National Laboratory, USA.
Z. Li, B. Dezillie

Bucharest, Institute of Nuclear Physics and Engineering, Romania
A. Vasilescu

Bucharest, Institute of Physics and Technology of Materials, Romania
T. Botila, D. Petre, I. Pintilie, L. Pintilie

Catania University, Italy
S. Albergo, D. Boemi, R. Potenza, A. Tricomi

CERN, Switzerland
F. Lemeilleur, G. Casse, M. Glaser, C. Leroy, P. Riedler,
S. Roe, A. Ruzin, P. Weilhammer, K. Zankel

Demokritos, Institute of Nuclear Physics, Greece
G. Fanourakis, D. Loukas, A. Markou, I. Siotis, S. Tzamarias, A. Vayaki

Dortmund University, Germany
R. Wunstorf, F. Huegging

Fermilab, Batavia (IL), USA
S. Kwan, D. Anderson

Firenze University, Italy
M.Bruzzi, U. Biggeri, E.Borchi, E.Catacchini, E. Focardi, G. Parrini

Gent University, Belgium
P. Clauws

Glasgow University, U.K.
K. Smith, R. Bates, S. Manolopoulos, V. Oshea, A. Pickford, C. Raine

Hamburg University, Germany
G. Lindstroem, E. Fretwurst, M. Kuhnke, M. Moll

Karlsruhe University
W. de Boer, G. Grigoriev, S. Heising, D. Knoblauch,

Kiev, Institute for Nuclear Research, Academy of Sciences, Ukraine
P. Litovchenko

Lancaster University, UK
T. Sloan, L. Beatty, T. Brodbeck, A. Chilingarov, G. Hughes, P. Ratoff, B.K.Jones, S. McGarry, M.Mcpherson

Liverpool University, U.K.
P. Allport, M. Hanlon

London, Brunel University, UK
S. Watts, A. Holmes-Siedle, M. Ahmed, M. Solanky

London, Imperial College, UK.
G. Hall, B. MacEvoy

London, Kings College, UK
G. Davies

Ljubljana, J. Stefan Institute, Slovenia
V. Cindro, M. Mikuz

Modena University, Italy
G. Ottaviani

Munich, Max Planck Institute, Germany
G. Lutz, R.H. Richter

Munich, Technischen Universitaet Muenchen, Germany
C. Da Via

Padova University, Italy
D. Bisello, N. Bacchetta, A. Giraldo

Perugia University, Italy
G.M. Bilei, P. Bartalini, P. Ciampolini, D. Passeri, A. Santocchia

Pisa, INFN, Italy.
G. Tonelli, R. Dell'Orso, A. Messineo, P. Verdini, R. Wheadon

Prague, Nuclear Center of Charles University
I. Wilhelm

Prague, Czech Technical University, Czech Republic
B. Sopko, S. Pospisil

Prague, Institute of Physics, Academy of Sciences, Czech Republic
V. Vrba, P. Sicho

Stockholm, Royal Institute of Technology, Sweden
B. Swenson

St Petersburg, Ioffe Physico-Technical Institute, Russia
E. Verbitskaya, V. Eremin

Villigen, PSI, Switzerland
K. Gabathuler, R. Horisberger

Warsaw, Institute of Electronic Materials Technology (ITME), Poland
Z. Luczynski, E. Nossarzewska, P. Zabierowski

Warsaw, Institute of Electron Technology (ITE), Poland.
M. Wegrzecki, W. Slysz

Associated Companies:

Canberra Semiconductor, Belgium
P. Burger

Micron Semiconductor, U.K.
C. Wilburn

SINTEF, Norway
B. Sundby Avset

Observers:

European Space Agency, ESTEC, Solar System Division, Holland
B. Johlander

IMEC, Belgium
C. Claeys, E. Simoen

Max Planck Institute, Munich, Germany
J. Kemmer, N. Meidinger

1. INTRODUCTION

This is the second status report of the RD48 or ROSE Collaboration. The first status report was issued in 1997, reference [1]. The Collaboration is concentrating on the problems of bulk damage in silicon resulting from irradiation by hadrons. The main scientific results are outlined, especially those that have important implications for the LHC detectors and are relevant to the future plans of the collaboration. It is now clear that one of the key damage parameters can be improved. Further work over the next year will be needed to develop and commercialise a suitable material. For detailed information, references are made to the relevant paper, technical note or workshop talk. A Workshop will be held at CERN from 2^{nd} – 4^{th} December 1998 when many of the results contained in this report will be discussed further, together with many other findings that have only been referenced briefly. Recommendations are made concerning the choice of material for silicon trackers that are to be used in harsh radiation environments.

2. THE ROSE COLLABORATION - OVERVIEW

The ROSE Collaboration consists of international groups working on detectors for particle physics experiments at the LHC. In addition, the Collaboration benefits from the very valuable input of solid state physicists and the expertise of silicon manufacturers. The Collaboration formed following the First Workshop on Radiation Hardening of Silicon Detectors, at CERN in October 1995. The proposal [2] was approved by the LHCC in June 1996. The Second Workshop was held at CERN in February 1997. The Third Workshop was held at DESY in February 1998. As noted above, the fourth Workshop will be held shortly. A World-Wide-Web page also provides useful information [3].

The close involvement of Canberra, Micron and SINTEF is shown through their "Associated Company" status.

Work at ITME and ITE in Poland has been vital for the rapid development, production and processing of the various materials.

The objectives of the collaboration are,

a) To develop radiation hard detectors that can operate beyond the limits of present devices and that ensure guaranteed operation for the whole lifetime of the LHC experimental programme.

b) To make recommendations to experiments on the optimum silicon for detectors and quality control procedures required to ensure optimal radiation tolerance.

The key idea is that one can improve the radiation tolerance of silicon by defect engineering. Defect engineering involves the deliberate addition of impurities to silicon in order to effect the formation of electrically active defect centres and thus control the macroscopic parameters of devices. If current models are correct, then the key ingredients to change are oxygen and carbon. Oxygen and carbon capture silicon vacancies and interstitials respectively. The carbon is converted from a substitutional to an interstitial position which is mobile at room temperature. It eventually forms stable defects with oxygen and substitutional carbon. Diffusing silicon interstitials and vacancies escape from a region of silicon where an intense concentration of Frenkel pairs are produced by a Primary Knock-On Atom (PKA). The PKA is produced by the incident radiation. Vacancies can react with one another to

form multivacancy defects. This leads to clustering of intrinsic defects around the PKA production point. This so-called “cluster” region controls many of the electrical parameters of irradiated silicon.

Various types of silicon are being evaluated with resistivities above 500 ohm cm. These are high resistivity epitaxial, FZ Si-Ge, FZ Si-Tin, carbonated FZ and oxygenated FZ. Oxygenated FZ has been grown using gas doping by Polovodice in Prague. However, oxygen concentrations greater than about 10^{16} cm^{-3} are not possible with this method. ITME in Poland have recently grown highly oxygenated FZ using a "jet" technique - this involves a quartz ring plus oxygen gas jet around the float-zone. ITME in Poland have also grown high resistivity epitaxial layers as thick as 200 μm. MACOM in the USA have grown epitaxial layers up to 150 μm thick. CZ material has also been studied. Tin doped material is important to study. Ref. [4] shows that tin highly suppresses divacancy production. Both Topsil and ITME have grown Si-Tin FZ. In both cases, the tin concentration was about 2 to 3 10^{17} cm^{-3}. Standard material with high oxygen content was also achieved by diffusion of oxygen from a thick oxide layer. This “oxygen diffused” material was made by ITE. Figure 1 shows that most of the oxygen/carbon concentration variants have been made. Infra-red absorption and Secondary Ion Mass Spectroscopy (SIMS) have been used to obtain these concentrations in float zone material. Epitaxial layers have been studied using SIMS. Photoluminescence has proven to be the best technique for checking the level of compensation.

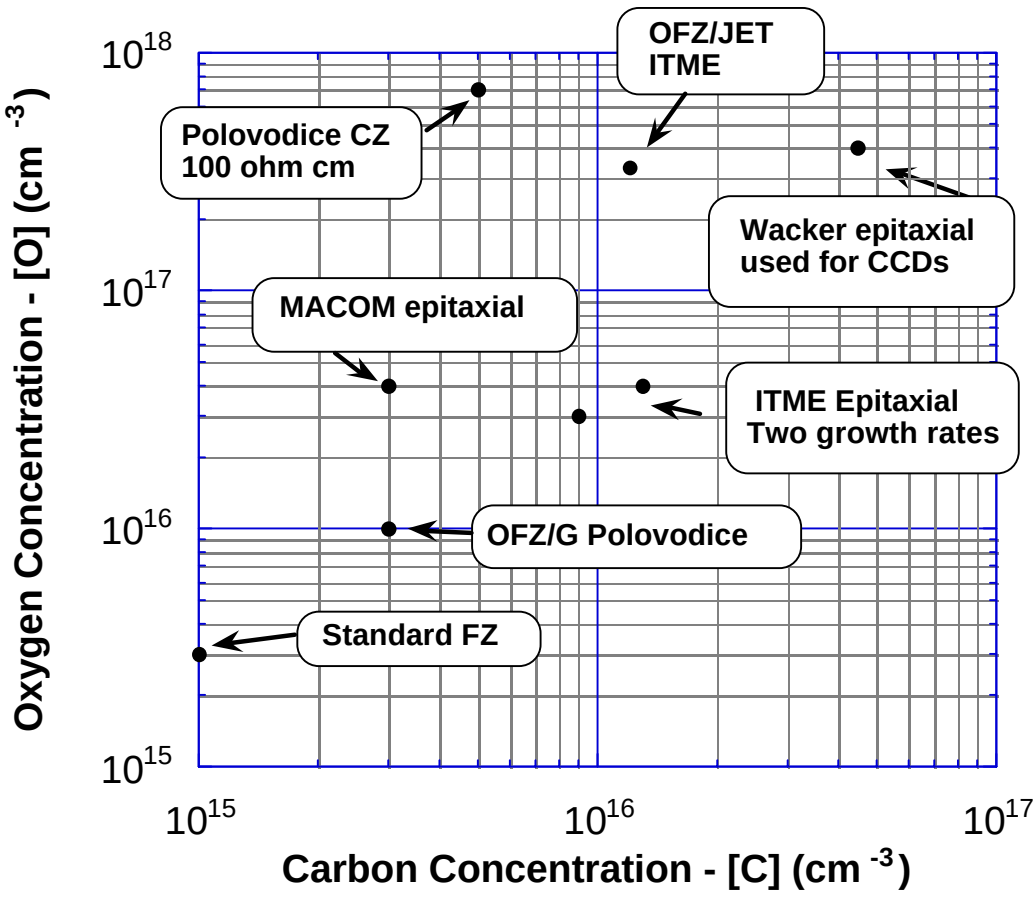

Figure 1 Oxygen and carbon concentrations in substrates investigated by the ROSE Collaboration.

The current status of the work is summarised in Table 1. Testing is in three categories: material characterisation, defect characterisation and macroscopic characterisation after irradiation (IV, CV etc.). "I" means "In progress", Y means "Finished", N means " To be done" .

Table 1 Status of materials under investigation by the ROSE Collaboration.

Material	**Manufacturer**	**Made**	**Tested See above**
Standard FZ	Wacker + others	Y	YYY
Epitaxial	MACOM	Y	YYY
Epitaxial	ITME	Y	YYY
FZ+ O OFZ/Gas	Polovodice	Y	YYY
FZ + C	Polovodice	Y	YIY
FZ + N	Polovodice	Y	YIY
FZ+ O + C	Polovodice	Not Made	
FZ+ 0.1% Ge	Topsil	Y	YYY
FZ+ Sn	Topsil/Aarhus	Y	YNY
FZ + Sn	ITME	Y	YIY
FZ + O OFZ/Jet	ITME	Y	YNY
CZ 100 ohm.cm	Polovodice	Y	YYY
FZ + O Diffused	ITE	Y	YNY
FZ + C Diffused	ITME	Y	NNN

3. MACROSCOPIC EFFECTS

This section provides a brief overview of radiation effects in silicon detectors to make the document self-contained and provide a reference for the results given in Section 4.

Four main macroscopic effects are seen in high-resistivity diodes following irradiation by MeV neutrons. The diodes are usually processed on 300 μm thick n-type material with a resistivity of around 4 kΩ cm. Similar effects are also seen following GeV proton and pion irradiation which also create cluster type damage. Macroscopic changes are found to scale with the Non-Ionising Energy Loss (NIEL). This has been calculated and can be used to relate the damage caused by particles of different types and energies. Thus, one needs only to refer to an equivalent 1 MeV neutron fluence. For brevity, this paper will use the term "fast neutrons" rather than "1 MeV equivalent neutron" when quoting fluences. A compilation of recommended NIEL values to use for various particles over a wide range of energies is given in reference [1].

The various macroscopic effects seen in neutron irradiated silicon are described in the following sections together with a discussion of the complex room temperature annealing behaviour.

3.1 Effective Doping Changes

In a non-irradiated diode the space-charge results from shallow dopants in the silicon. Irradiation results in a build-up of negative space-charge in depletion regions due to the introduction of deep levels. The effective doping concentration, N_{eff}, is inferred from the voltage required to obtain full depletion, V_{FD}, which is,

$$V_{FD} = \frac{(thickness)^2 \cdot e \cdot |N_{eff}|}{2 \cdot \varepsilon_0 \cdot \varepsilon_{Si}} \qquad (1)$$

In equilibrium - no external bias - both n-type and p-type material become almost intrinsic after around 10^{13} cm^{-2} fast neutrons. However, under bias, the effective doping concentration is entirely controlled by radiation induced deep levels for fluences beyond 10^{13} fast neutrons cm^{-2}. In an n-type diode, deep acceptors eventually cause the depletion region to grow from the n+ rather than p+ contact. The fluence at which this occurs is referred to as the "inversion fluence". Fig. 2 illustrates that a detector which starts with a positive space charge - point B - has a negative space charge following irradiation - point A. The inversion point is marked as N_{eff} = Zero.

It is important to note that CMS have found that heavily irradiated detectors must be biased by about twice the depletion voltage to give maximal signal to noise performance.

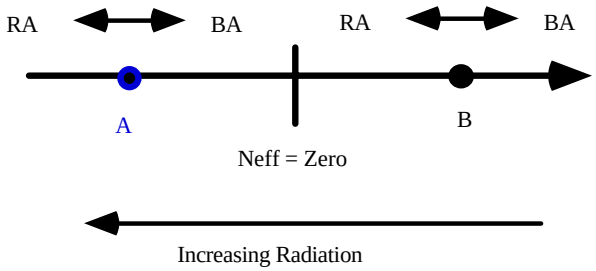

Figure 2 Changes in the effective space charge, N_{eff}, in the depletion region of diodes irradiated by fast neutrons. BA and RA refer to the beneficial and reverse annealing processes that occur after irradiation. N_{eff} is represented as a point on the axis.

3.2 Diode Leakage Currents

Diode leakage currents increase significantly and anneal following irradiation by about 50 percent over a period of about two weeks at room temperature. The radiation induced leakage current in a detector is defined in terms of the parameter α. This is the leakage current increase, ΔI, per unit volume per incident particle fluence, ϕ, or,

$$\Delta I/\text{Volume} = \alpha\phi \qquad (2)$$

α is around $(4 - 9)\ 10^{-17}$ A cm^{-1} immediately after irradiation.

3.3 Reverse annealing of the effective space-charge

Following irradiation to high fluences, the build-up of negative space-charge is seen to increase dramatically after several months for diodes kept at room temperature. This can be suppressed by keeping the diodes at about -5 ^{o}C. This is called "reverse annealing". The best fit to the data is found using a second-order process parameterisation [1]. However, the rate constant has been found to be fluence dependent. This means that a first-order disassociation or re-ordering process is responsible. The activation energy is 1.31+/- 0.04 eV. It takes several years for the process to saturate at room temperature. It can be accelerated by heating samples at 80 - 100 ^{o}C. The amount of reverse annealing is proportional to the irradiation fluence.

3.4 Charge collection efficiency

Silicon detectors are used to detect charged particles. These traverse the silicon producing about 24,000 electron-hole pairs in a 300 μm thick detector. At room temperature, about 10% of the charge is lost per 10^{14} fast neutrons cm^{-2}. Recent experimental measurements [5] find that for temperatures below 100 K, fifty percent of the charge is recovered in detectors irradiated to 2 10^{15} neutrons cm^{-2}. The charge collection efficiency is still poor at 195 K. This has been referred to as the Lazarus effect. In effect, the defects are frozen out. What is surprising is that there is still charge loss at 4 K.

3.*5 Annealing effects*

Both the leakage current and the effective space charge anneal at room temperature following irradiation by fast neutrons. There is a beneficial recovery which occurs over about two weeks followed by the reverse annealing stage referred to above. The beneficial annealing stage affects both the leakage current and effective space charge. Reverse annealing only occurs to the effective space charge. The leakage current continues to anneal for years after irradiation. One can write the effective space charge in an initially n-type substrate as,

$$N_{eff} = N_{eff,0} - N_S - N_{BA} - N_{RA} \qquad (3)$$

where $N_{eff,0}$ is the starting doping concentration, N_S is the stable concentration of radiation induced defects, N_{BA} is the concentration of radiation induced defects that anneal out over a two week period at room temperature, and N_{RA} is the concentration of radiation induced defects that anneal in over several months at room temperature. The fast neutron introduction rate for these concentrations are roughly 0.025, 0.015 and 0.06 cm^{-1} for N_S, N_{BA} and N_{RA} respectively. The introduction rate for N_S is referred to as the **β parameter**. Some confusion can arise because the depletion voltage depends on the magnitude of N_{eff} and not its sign - note equation (1). This is illustrated in Fig. 2. Take point B. This corresponds to a material which is initially n-type and has not been irradiated beyond the inversion point. Beneficial annealing will cause the depletion voltage to increase. If one now takes point A which corresponds to a material that has been irradiated past the inversion point, the same annealing process will cause the depletion voltage to decrease. Similar comments also apply to the effect of the reverse annealing process on the depletion voltage.

3.6 The Bottom Line

Four key parameters describe the behaviour of the irradiated silicon detectors and determine their lifetime and operating conditions in high radiation environments. These parameters are:

a) The leakage current parameter, α.
b) The introduction rate for stable acceptors, β. This controls the operating voltage after the inversion fluence leading eventually to breakdown.
c) The inversion fluence. This is proportional to the initial doping concentration, $N_{eff,0}$.
d) The introduction rate for the space-charge responsible for reverse annealing. This process can be inhibited by cooling the detector.

Finally, the charge collection efficiency is degraded for fluences beyond about a few 10^{14} n cm^{-2} due to trapping.

4. SUMMARY OF KEY RECENT RESULTS

This section provides a summary. More details can be found in the relevant references. Progress has been made in two areas – new materials and in operating conditions. These are discussed in the following sections.

4.1 Material Development

With the **important exception** of the β parameter, it has proven difficult to achieve major changes to the fast neutron induced macroscopic parameters by altering impurity levels. However, substrates with high oxygen content are considerably less affected by gamma irradiation compared to standard float-zone material as is shown in Fig. 3. In this case no cluster region is formed. This means that the behaviour of neutron irradiated silicon is dominated by defect clusters. Silicon-tin should perform much better. The material tested to date only shows a small effect. However, it is likely that there is a threshold to the tin concentration before a dramatic reduction is seen in the divacancy production. In reference [4], the tin concentration was at least 10^{18} cm^{-3}.

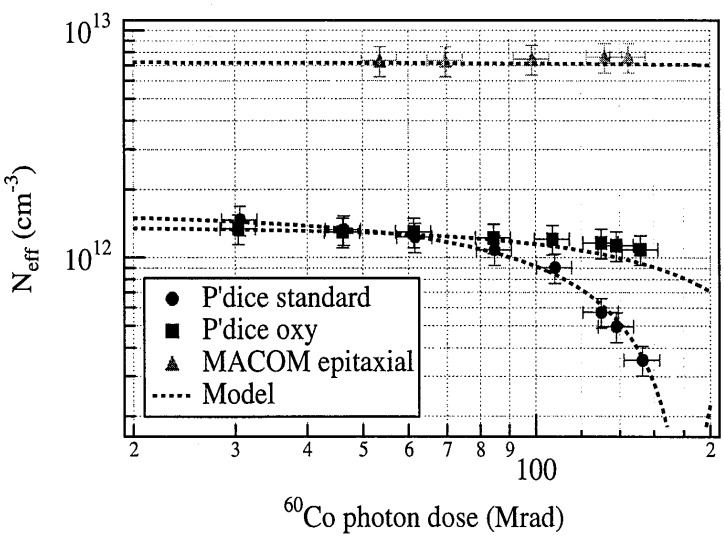

Figure 3 Effective doping changes caused by gamma irradiation of various silicon materials, [6].

Some substrates show important differences compared to standard Float-Zone material. For instance, some MACOM epitaxial material shows effective doping changes after inversion that are a factor three better than normal – i.e. the β parameter is substantially lower. This is a significant improvement and is being studied further. The most probable explanation for the improvement is due to the fact that the material is highly compensated - boron is removed at a faster rate than phosphorus resulting in a positive space charge that balances the radiation induced negative charge. There is also clear evidence that high carbon concentrations make the material less radiation tolerant. Finally, in CZ material, reverse annealing changes are a factor two less - Fig. 4, [7]. However, higher resistivity material is needed for detectors and this is being pursued. Reverse annealing has been linked to the photoluminescence W-line, [1]. A recent paper has found that this line is reduced in high [O] material, [8]. This is consistent with the CZ result and provides some hope that the microscopic cause of reverse annealing may be understood in the near future.

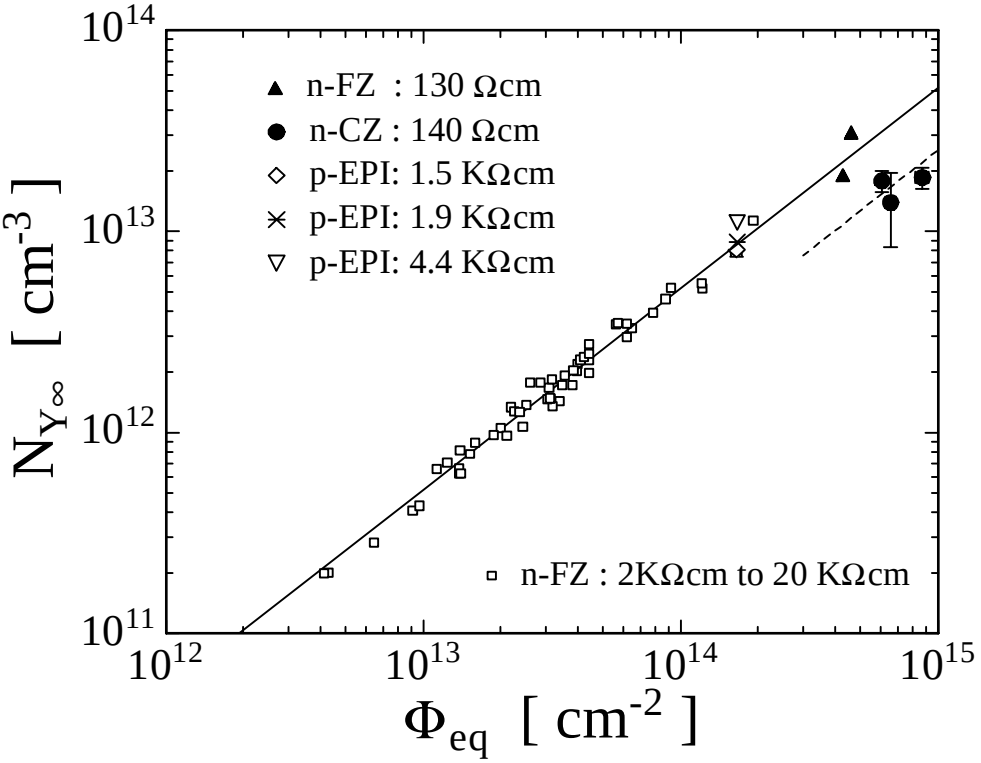

Figure 4 Reverse annealing damage parameter for various materials and fluences, [7].

The leakage parameter, α, has been found to be material independent as shown in Fig. 5. Defect clusters appear to be the main microscopic cause of the leakage current. Note that α may be slightly lower at higher fluence. This might be caused by defect clusters capturing vacancies at high fluences – see Section 5.1.

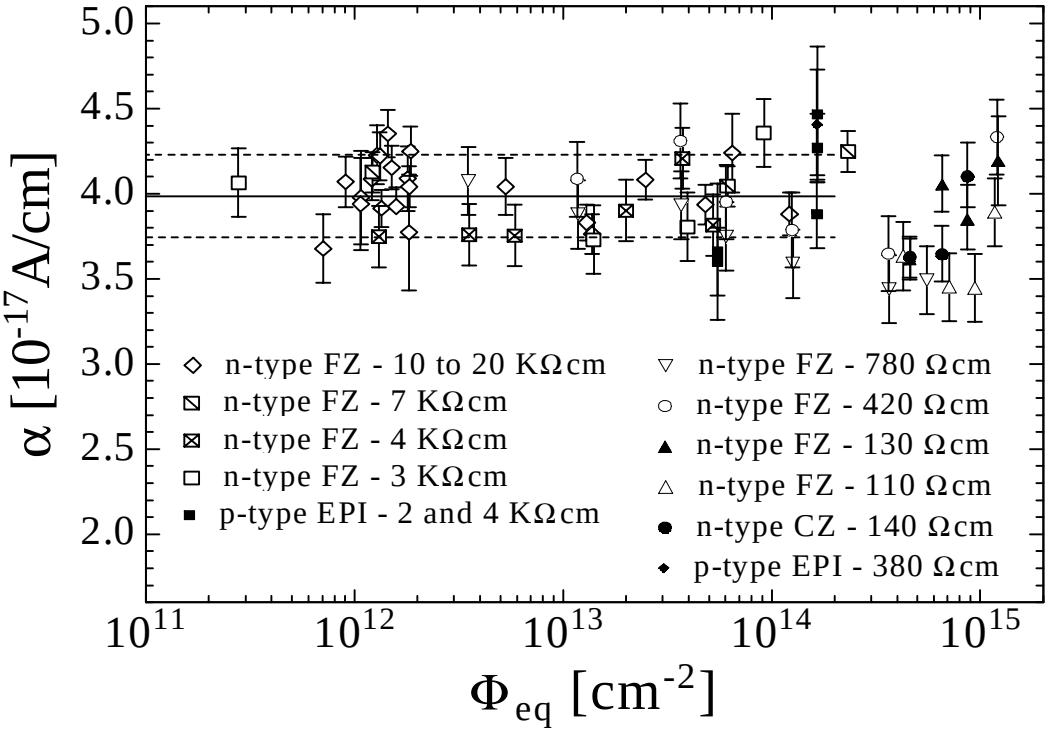

Figure 5 Leakage current damage parameter for various silicon substrates, [9].

As mentioned earlier, the one parameter that can be altered, and ultimately controlled, is the β parameter. This parameter for various substrates is shown in Table 2. Note that this parameter scales with NIEL for standard material. It does not for some substrates as is shown in Fig. 6. This is being studied further.

Table 2 The β parameter in various substrates, [10].

Material	β (cm^{-1}) 1 MeV neutrons	β (cm^{-1}) 24 GeV/c protons
Standard FZ(Polovodice) ITE processed	**0.028**	**0.016**
Standard FZ (Polovodice) SINTEF processed	-------	**0.012**
Oxygen Jet FZ	**0.020**	**0.005**
MACOM Epitaxial	**0.007**	**0.006**
Carbon enriched FZ	**0.028**	**0.033**
Si-Tin	**0.020**	-------
ITME Epi I Note 1	-------	**0.018**
ITME Epi II Note 1	-------	**0.011**
Standard FZ from Silicon Valley Microelectronics Inc.	-------	**0.008**

Note 1: Similar resistivity but one has 10% higher [P].

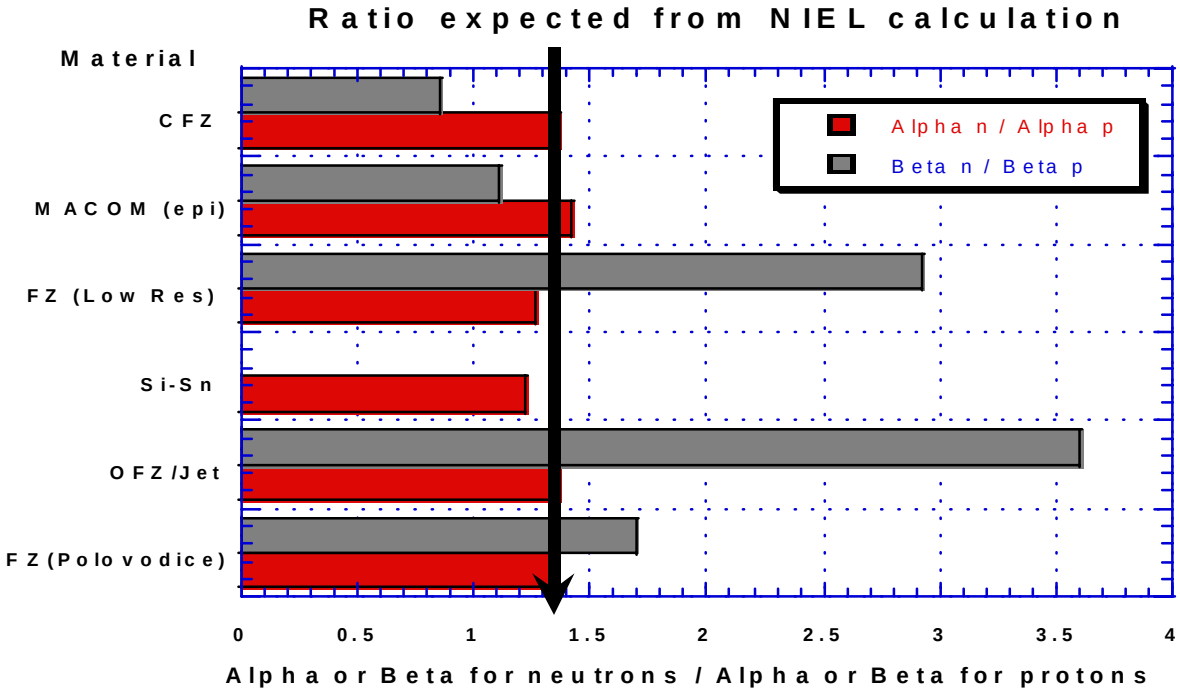

Figure 6 Ratios of damage parameters between reactor neutrons and 24 GeV/c protons in various silicon substrates.

Note that diodes processed on the same material by ITE and SINTEF show different values of β although results from more diodes are needed. Defect concentrations after proton irradiation in similar SINTEF diodes are also lower, [11]. Some process dependence appears probable.

Fig. 7 shows how the effective doping concentration varies as a function of irradiation for various substrates. The β parameter is extracted from such data. The diodes were heated for 4 minutes at 80 ^{o}C after each irradiation step. This is very important. This is equivalent to allowing the diode to undergo the 2 week beneficial annealing stage at room temperature. This ensures that the data is not affected by short term annealing effects. **Such a procedure is recommended for all such testing**. Note the excellent performance of the oxygen-jet material in the proton beam.

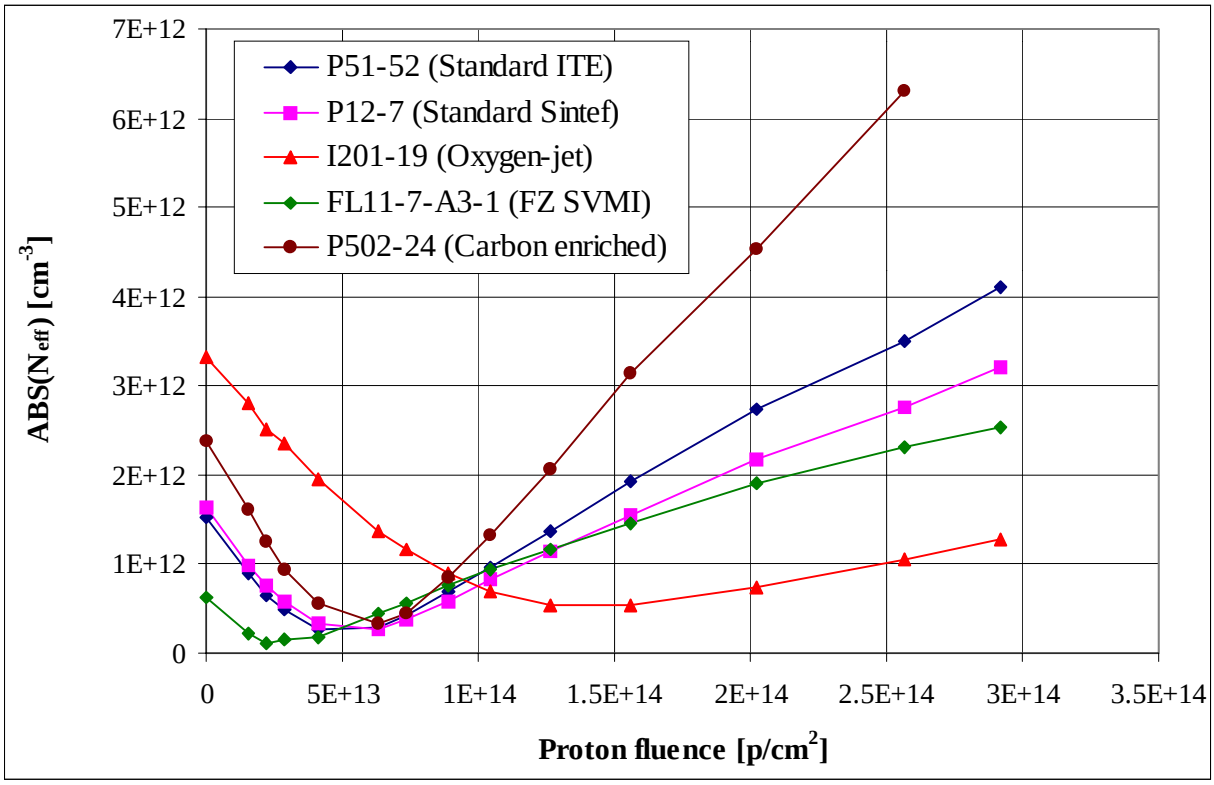

Figure 7 Effective doping change as a function of 24 GeV/c proton fluence for various substrates [10].

Fig. 7 also shows that the inversion fluence is directly proportional to the starting effective doping concentration. It has been found that, [10],

$$\phi_{Inversion} \approx 20 \times N_{eff,0} \qquad (4)$$

i.e. lower resistivity material inverts at a higher fluence.

4.2 Operating Conditions

It should be noted that improved tolerance to radiation effects has been achieved by the use of multi-guard structures. These allow much higher operating voltages to be applied. In addition, there have been two recent developments in this area, both aimed at operating silicon detectors after heavy neutron irradiation - beyond a few 10^{14} n cm^{-2}. These developments are:-

a) To operate heavily irradiated detectors under forward bias, [12]. The I/V characteristics of heavily irradiated silicon are almost ohmic - it is similar to GaAs in that it becomes a relaxation rather than a lifetime material. At 250 K the forward current is no worse than the radiation induced generation current. As a rule of thumb, the voltage required to obtain the same charge collection efficiency (CCE) under forward as compared to reverse bias is about a **factor ten** lower.
b) To cool the detector to below 100 K, as noted in Section 3.4. The CCE improves dramatically. This behaviour has been broadly understood, [13], but further work is needed. Operation up to fluences of 10^{16} n cm^{-2} may be possible under these conditions.

5. RADIATION DAMAGE MODELS

These describe defect formation and the modelling of irradiated silicon devices.

Section 5.1 updates the model given in the earlier report, [1], in order to understand recent results. This updated model is used in Section 5.2 for the case of compensated silicon.

5.1 Updated defect kinetics model

Much understanding of radiation effects can be achieved by numerical calculations of the evolution of complex defects formed during irradiation. The elementary defects produced are vacancies (V), interstitials (I) and divacancies (V_2). Divacancies are static until about 600 K whereas vacancies and interstitials are mobile except at very low temperatures. Those escaping initial recombination diffuse through the crystal reacting with other defects and impurity atoms, particularly oxygen and carbon. Reaction rates are controlled by the concentration of impurities and defects and their relative capture radii. Davies et al. [14] have explained infra-red absorption spectra of electron irradiated silicon by means of a small number of reactions. A kinetics model, based on this work and suitably extended, has been used to predict the evolution of defects during neutron irradiation [15]. The main reactions, which include those of interstitial and substitutional carbon (C_i and C_S) are listed in Table 3. Reactions that have been included since the last report, [1], are shown in **bold type**.

Table 3 Main reactions in defect kinetics modelling

I Reactions	**V reactions**	**C_i Reactions**
A) Diffusion reactions		
$I + C_s \rightarrow C_i$	$V + O \rightarrow VO$	$C_i + C_s \rightarrow CC$
$I + V_2 \rightarrow V$	$V + P \rightarrow VP$	$C_i + O \rightarrow CO$
$I + VP \rightarrow P$	$V + VO \rightarrow V_2O$	$CO+I \rightarrow COI$ *
$I + V_3O \rightarrow V_2O$	$V + V_2O \rightarrow V_3O$	$CC+I \rightarrow CCI$ *
$I + B_s \rightarrow B_i$		**$B_i + C_s \rightarrow BC$** **$B_i + O \rightarrow BO$** **$B_i + B_s \rightarrow BB$** *Not thought to be electrically active
B) Reactions in PKA region		
$I + V \rightarrow Si$ (annihilation)	$V + V \rightarrow V_2$	
$I + I_N \rightarrow I_{N+1}$ (See text) +	**$V + V_N \rightarrow V_{N+1}$ (See text) +**	**+ May occur for diffusing vacancies and interstitials - reactions A) - after heavy neutron irradiation.**

Reactions (A) are for vacancies and interstitials diffusing throughout the crystal. Reactions (B) only have a significant chance of occurring during a Primary Knock-on Atom (PKA) cascade. The densities of primary defects in the small volume of the displacement damage region are large compared to impurity atom concentrations in the high resistivity silicon. For this reason the relative introduction rate of V_2 in neutron irradiation is greatly in excess of that in electron irradiation. The (B) reactions occur over a short period following the production of the PKA. It is now clear that one should add interstitial reactions forming multi-interstitial defects. Clustering is favoured for both interstitials and vacancies. Reference [16] has calculated the binding energies of clusters of either

vacancies or interstitials up to size 5 - it shows that a cluster of size N + 1 is more stable than one of size N for N less than or equal to 5. Reference [17] has also performed calculations for multivacancy defects. It confirms that multivacancy defects are stable and in addition shows that the V_6 or hexavacancy is the most stable configuration. A further consequence of these calculations is that for fast neutron fluences beyond 10^{14} cm^{-2}, multivacancy defects in clusters will start to compete with oxygen for the diffusing vacancies.

For quantitative calculations the oxygen, carbon, phosphorus and boron concentrations ([O], [C], [P] and [B]) and introduction rates of I, V and V_2 are required. Introduction rates of I, V and V_2 due to neutron irradiation calculated from DLTS measurements are of order one cm^{-1} . Ratios of capture radii are reasonably well known, e.g. Davies et al. [14]. Because of its concentration and capture radius, oxygen is the dominant capture site for vacancies; carbon behaves similarly as a sink for interstitials.

5.2 Defect kinetics in compensated silicon

Until recently, defect kinetics reactions in n-type silicon involving boron were thought to be irrelevant. However, it is now realised that because the ratio of the capture radius for silicon interstitials by boron compared to carbon is large (10 to 40), that even low boron concentrations can be important. Moreover, there are roughly three times more diffusing silicon interstitials than vacancies due to cluster formation near the PKA. This is especially relevant if the material is compensated. Normally, high resistivity silicon is only lightly compensated. However, recent DLTS measurements on epitaxial diodes can only be explained if the material is compensated, [11]. If phosphorus in the material is removed by irradiation at a slower rate than boron, then the positive space-charge increases and balances the radiation induced negative space-charge. This can explain many of the different β values that have been obtained. An important consequence is that, with care, this parameter can be controlled and significantly reduced. This would substantially reduce the final depletion voltages of detectors after 10 years operation at the LHC. It is simple to show that after inversion for material in which [P] << [O], and [B] << [C], then

$$\beta \approx -\frac{[P]}{[O]} \times \frac{R(P,V)}{R(O,V)} \times r_v + \frac{[B]}{[C]} \times \frac{R(B,I)}{R(C,I)} \times r_I - r_S \quad . \qquad (5)$$

r_v and r_I are the introduction rate of diffusing vacancies and interstitials respectively. These are 0.63 and 1.5 cm^{-1} respectively. r_s is the introduction rate for the stable radiation induced space charge, which is about 20 10^{-3} cm^{-1}. The R(X,Y) terms are the capture radii for the various reactions. Only the ratio for these reactions are needed. The R(P,V)/R(O,V) ratio is 14. The R(B, I)/R(C, I) ratio is not well known. It is known to be large – in the region of 10 to 40. Fig. 8 shows how β varies as a function of the [B]/[P] ratio for various oxygen and carbon concentrations. Fig. 9 is the same graph for a larger R(B, I)/R(C, I) ratio. Clearly a better knowledge of this ratio is required. Fig. 10 is similar to Fig. 8 except that lower resistivity material is assumed.

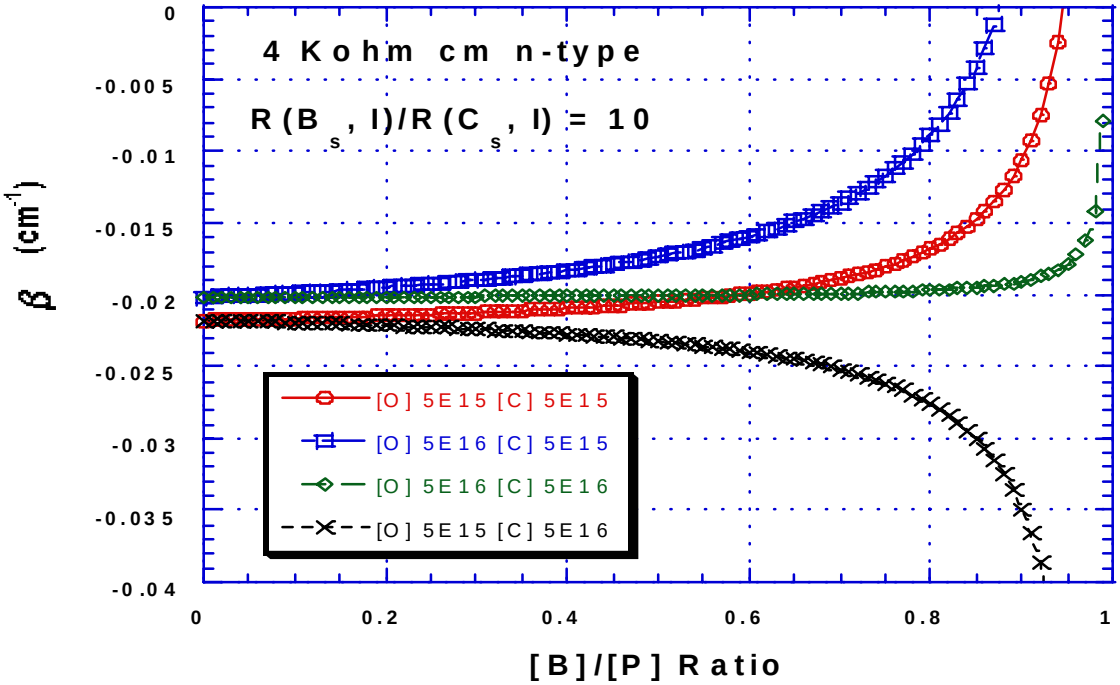

Figure 8 Calculated β parameter as a function of the boron to phosphorus ratio for various oxygen and carbon concentrations. The R(B, I)/R(C, I) ratio is 10. High resistivity material.

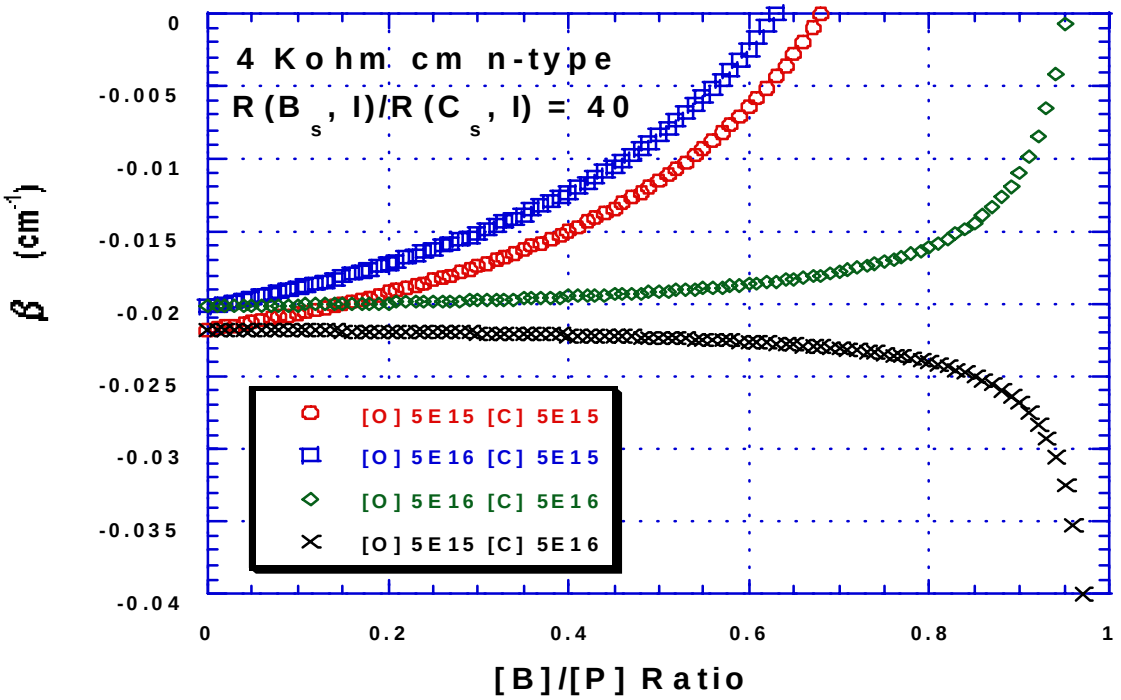

Figure 9 Calculated β parameter as a function of the boron to phosphorus ratio for various oxygen and carbon concentrations. The R(B, I)/R(C, I) ratio is 40. High resistivity material.

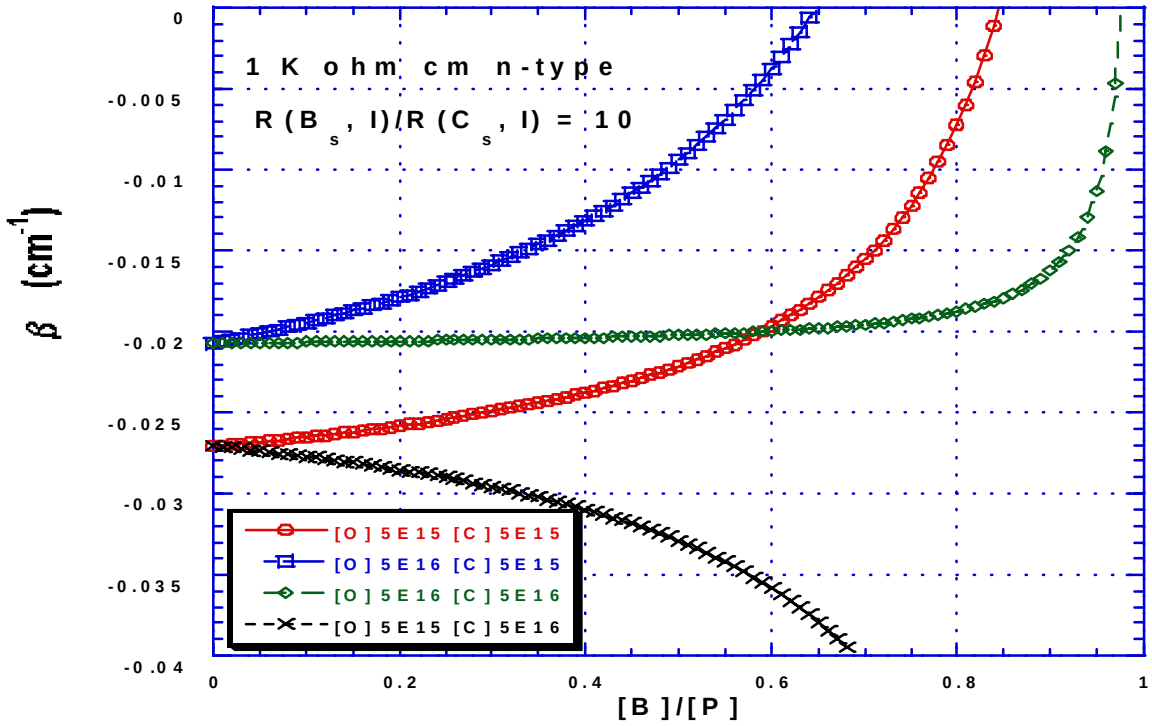

Figure 10 Calculated β parameter as a function of the boron to phosphorus ratio for various oxygen and carbon concentrations. The R(B, I)/R(C, I) ratio is 10. Low resistivity material.

The following conclusions can be drawn from these figures:

a) β is very sensitive to the compensation level. The lower resistivity material shows more sensitivity.
b) The sensitivity is reduced if the carbon and oxygen concentrations are similar.
c) If the [O]/[C] ratio is greater than 1, then β reduces for more highly compensated material. It is possible to "defect engineer" low β material.
d) If the [O]/[C] ratio is less than 1, then β increases for more highly compensated material. This explains why substrates with high carbon levels show worse radiation tolerance.

5.3 Device Modelling

3D device modelling of irradiated silicon detectors using a modified HFIELDS simulator which includes deep levels has been implemented by the Perugia group– reference [18].

6. HARDNESS FACTORS

Damage projections for the trackers need reliable and consistent Non-Ionising Energy Loss (NIEL) information. The NIEL information given in [1] should be used. The leakage current parameter is an excellent way to compare the hardness factor of various radiation sources – see ref. [9] for further details. The hardness factor for 24 GeV/c protons is confirmed as being 0.51+/-0.01, [9]. Results mentioned in Section 4. 1 indicate that the β parameter in non-standard silicon substrates does not scale with NIEL – GeV protons are **less** damaging in OFZ/Jet material than expected. This needs to be understood.

7. CONCLUSIONS

The following conclusions can be drawn from the data that has been collected over the last year or so:

a) The β parameter can be reduced by at least a factor of 2 to 3. If this can be achieved reliably then this will provide safe operation of the detectors in the LHC experiments over a ten year period. The reason for the lower β parameter, in most cases, is thought to involve the compensation level of the material and the oxygen and carbon concentrations. To oversimplify the recipe for such a material, it needs to be suitably compensated and the oxygen/carbon ratio must be greater than one.

b) The compensation level of the starting material is important for all silicon substrates and should be checked before it is used for detector production. This is possible using photoluminescence.

c) Low resistivity (1 Kohm cm) material should be used. This inverts at a higher fluence and reduces the final operating voltage after 10 LHC years, [1]. Recent results from CMS, [19], confirm this conclusion. ATLAS, [20], find no improvement. This may be due to the compensation level in the material and needs urgent further study.

d) Some possible process dependence has been observed. The reason for this is not clear. It may be difficult to elucidate the reason due to commercial considerations.

e) Oxygenated FZ made using the jet technique performs better than standard FZ if irradiated with protons. The material needs to be studied with charged pions and the reason for the NIEL violation (compared to neutrons) needs to be understood. Diffused oxygen material has been tested using neutrons and showed no improvement. This material will be tested using protons.

f) Silicon-tin has yet to prove itself. Tin concentrations beyond 10^{18} cm^{-3} at least are needed. It is not trivial to make such material with the required resistivity.

g) CZ material looks promising and higher resistivity substrates are being investigated – e.g magnetic CZ. The reduction of the reverse annealing by a factor 2 is not understood, but gives some hope that this process may be understood and controlled.

h) Cryogenic operation looks to be a very promising way to operate silicon detectors after very high neutron fluences. Further work is needed to understand such operation and develop low mass cryogenic systems. Forward operation also needs further investigation. Both the RD39 and RD48 collaborations are investigating this operational mode in more detail. Various silicon substrates will be tested at cryogenic temperatures - some may perform better if used at 100 K.

i) Irradiation testing of detectors needs careful planning. The “irradiate and anneal method” outlined in Section 4 should form the basis of an agreed standard procedure.

j) The leakage current can be used to compare the hardness of various radiation sources. Due to annealing effects, suitable procedures should be followed – cf. Section 4.

8. FUTURE WORK

From the conclusions in Section 7, the following work is proposed:

a) To complete testing of materials – specifically, highly carbonated silicon, Si-Tin with higher tin concentration and increased resistivity, higher resistivity CZ (magnetic CZ).

b) To develop low-β material, and look in detail at the effect of compensation on the material hardness. **This is an issue that needs urgent study**. It should be possible to make low-β material reliably and consistently by epitaxial growth and/or by using the precise control on the phosphorus concentration that can be achieved with the Neutron Transmutation Doping (NTD) technique.

c) To study the radiation tolerance of highly oxygenated FZ with charged pions and diffused oxygen FZ material with charged particles.

d) To understand in more detail the behaviour of irradiated silicon at low temperature (100 K).

9. IMPLICATIONS FOR THE LHC DETECTORS.

Table 4 provides a simplified overview of various choices for silicon detectors in high radiation environments. Note that pixel detectors can withstand higher fluences as the leakage current and noise levels per element are lower

Table 4: Overview of material and operating choice for silicon detectors in harsh radiation environments.

Material or Operation	Maximum Fluence n cm^{-2}	Comment
Standard High Resistivity FZ (4 kOhm cm)	Strips 10^{14} Pixels 10^{15} (with partial depletion).	Guard Ring and high voltage operation needed. Operation marginal at the maximum fluence quoted.
Standard Low Resistivity FZ (1 kohm cm)	Strips 10^{14} Pixels 10^{15}	Operational safety margin to these fluences
β controlled material	Strips Few 10^{14} Pixels > 10^{15}	CCE will limit maximum fluence.
Cryogenic Operation (100 K)	Up to and beyond 10^{16} ?	More studies required.

10. MILESTONES

The status of the following milestones (LEB, 31 Oct. 1997) are as follows:

a) Decide on processing options for epitaxial and float-zone silicon.

This is a complicated issue. In addition, commercial interests make this a difficult area to have open discussions. Various results exist and many techniques have been tried (cf. Diffused oxygen). Most materials have been processed by three techniques – ion-implantation, diffused junction, MESA. The issue will be discussed at the next Workshop.

b) Evaluate hardness of detectors using highly oxygenated float-zone.

This has been achieved and has lead to very interesting results – Section 4. Plans for further work are mentioned in Section 8.

c) Evaluate hardness of Si-tin,and if promising clarify production possibilities.

Silicon-tin has been manufactured and tested. More work is needed to get higher tin concentrations and higher resistivity – cf. Sections 4 and 7.

d) Take active steps to raise awareness of RD48 results in the experiments by organising a Workshop in the first quarter of 1998, and to establish together with experiments, recommendations on materials (raw material, resistivity, and qualification procedures) and detector processing.

A Workshop was held at DESY in February 1998. Full details of the results given in this report will be presented at the next Workshop to be held at CERN, 2 - 4 December 1998. Testing of full-scale detectors made on low-resistivity material is in progress within ATLAS and CMS – cf. Section 7. A key result from recent work is that the compensation level of the raw material must be qualified – cf. Sections 5 and 7.

Proposed Milestones for future work are detailed in a separate document.

11. REFERENCES

1. RD48 Status Report, CERN/LHCC 97-39, June 1997.
2. ROSE Collaboration Proposal, CERN/LHCC 96-23, P62/LHC R&D, April 1996.
3. ROSE Web Page – http://www.brunel.ac.uk/research/rose/
4. B. Svensson et al., J. Appl. Phys. 72, 5616 (1992).
5. V. Palmieri et al., Preprint BUHE-98-06.
6. B. MacEvoy, 3rd Workshop on Radiation Hardening of Silicon Detectors, DESY, Hamburg, DESY-Proceedings-1998-02, February 1998.
7. G. Lindstrom et al., Paper presented at the 2nd Int. Conf. On Radiation Effects on Semiconductor Materials, Firenze, Italy, March 4-6 1998. To be published in NIM A.
8. M. Nakamura et al., Appl. Phys. Lett., 72 No 11, 1347 (1998).
9. M. Moll et al., Paper presented at the 2nd Int. Conf. On Radiation Effects on Semiconductor Materials, Firenze, Italy, March 4-6 1998. To be published in NIM A.
10. A. Ruzin et al., Paper presented at the 6th Int. Conf. On Advanced Technology and Particle Physics, Como, Italy, October 5-9 1998. To be published in NIM A.
11. M. Ahmed, Ph.D Thesis 1998, Brunel University. In preparation.
12. L. J. Beattie et al, Paper presented at the 8th Symposium on Semiconductor Detectors, Schloss Elmau, June 14-17 1998. To be published in NIM A.
13. S. J. Watts, High Resistivity Silicon Symposium Proceedings, ECS Meeting, Boston, Nov. 1998.
14. G. Davies et al., Semicond. Sci. Technol. 2, 524 (1987).
15. B. MacEvoy, Ph.D thesis, Imperial College. RAL-TH-97-003 (1997).
16. G. H. Gilmer et al., Nucl. Instr. and Meths. B102, 247 (1995).
17. J. L. Hastings et al., Phys. Rev. B 56, 10215 (1997).
18. CMS tracker TDR, CERN/LHCC 98-6, CMS TDR 5, April 1998.
19. G. Tonelli, VERTEX98, Santorini, Greece, Sept. 28 - 4 Oct 1998.
20. P. Allport, Private Communication.